Online Supporting Information for

Correlating the Chemical Composition and Size of Various Metal Oxide Substrates with the Catalytic Activity and Stability of As-Deposited Pt Nanoparticles for the Methanol Oxidation Reaction

Megan E. Scofield,[1] Christopher Koenigsmann,[1] Dara Bobb-Semple,[1] Jing Tao,[2] Xiao Tong,[3] Lei Wang,[1] Crystal S. Lewis,[1] Miomir Vukmirovic,[4] Yimei Zhu,[2] Radoslav R. Adzic,[4] and Stanislaus S. Wong[1,2,*]

*To whom correspondence should be addressed.

Email: stanislaus.wong@stonybrook.edu; sswong@bnl.gov

[1]Department of Chemistry, State University of New York at Stony Brook, Stony Brook, NY 11794-3400

[2]Condensed Matter Physics and Materials Sciences Department, Building 480, Brookhaven National Laboratory, Upton, NY 11973

[3]Center for Functional Nanomaterials. Building 735, Brookhaven National Laboratory, Upton, NY

[4]Chemistry Department, Building 555, Brookhaven National Laboratory, Upton, NY 11973

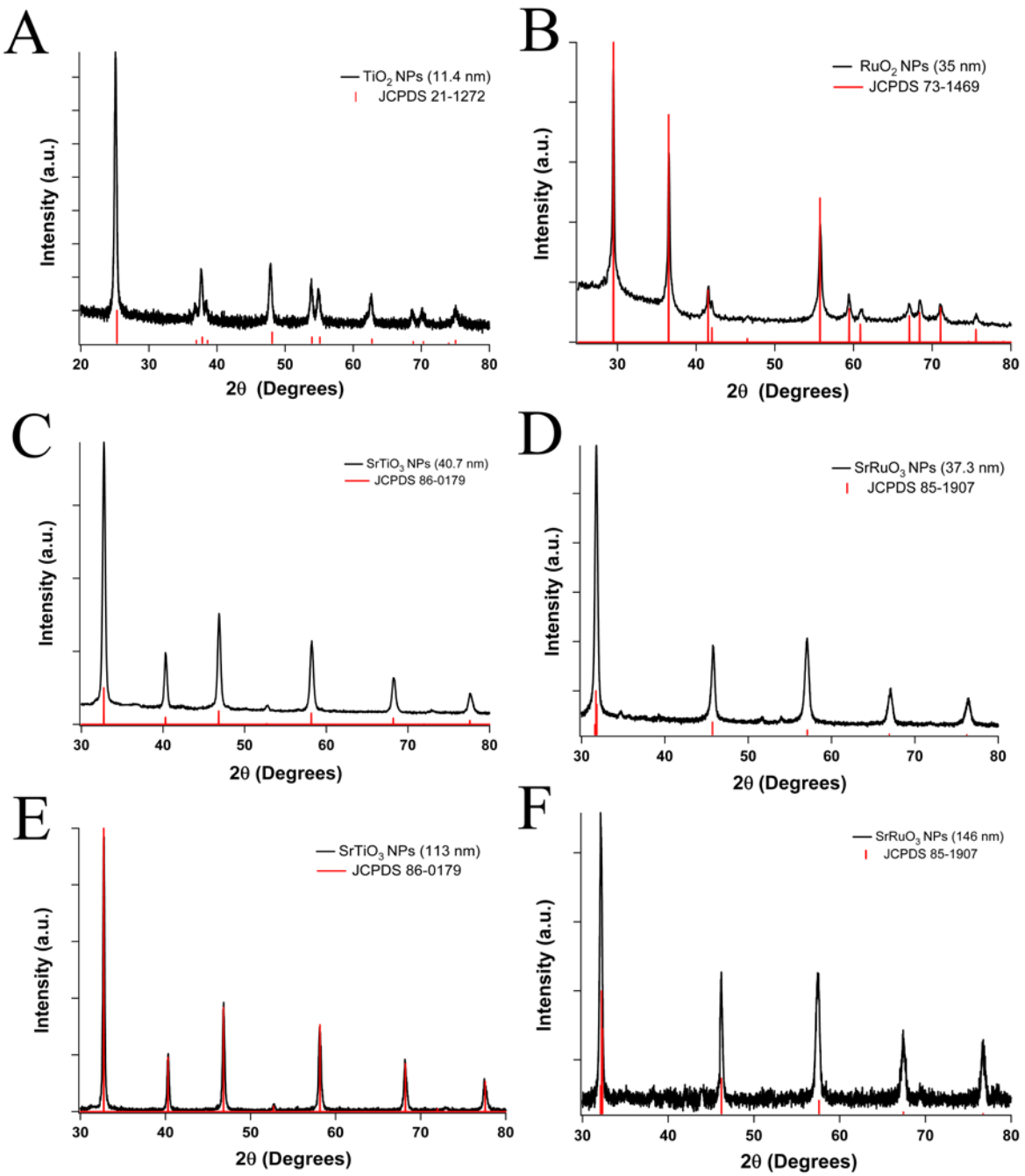

Figure S1. XRD patterns (black curves) for (A) TiO_2 NPs (11.4 nm), (B) RuO_2 NPs (35 nm), (C) $SrTiO_3$ NPs (40.7 nm), (D) $SrRuO_3$ NPs (37.3 nm), (E) $SrTiO_3$ NPs (113 nm), and (F) $SrRuO_3$ NPs (146 nm), respectively. All experimental peaks can be correlated with the expected assignments determined from individual JCPDS patterns, shown in red.

Figure 1 and Figure 2: Description of Characterization Analysis

Figure 1A consists of a TEM image. Overall, the TiO_2 particles exhibit a nanoparticulate morphology with an average size of 11.4 ± 2.8 nm. Figure 1B represents a high resolution TEM image in which the *d*-spacing was measured to be 3.57 Å, corresponding to the (101) plane of anatase TiO_2. Complementing the HRTEM image, an SAED pattern (Figure 1C) was also acquired, with the indexed rings further confirming the presence of the anatase structure.

Figure 1D is representative of our synthesized RuO_2 nanoparticles. The NPs possess an average diameter of 35 ± 3 nm. The HRTEM image seen in Figure 1E indicates a *d*-spacing of 3.13 Å, which corresponds to the (110) plane of RuO_2. A complementary SAED image observed in Figure 1F further attests to the desired composition, with the diffraction rings labeled.

Figure 2A highlights the uniformity of the size and shape of our 40 nm $SrTiO_3$ sample using SEM. Overall, the average particle size of the $SrTiO_3$ particles is 40.7 ± 0.7 nm. A higher resolution TEM image is present in Figure 2B, with the observed *d*-spacing of 2.81 Å attributable to the (110) plane of $SrTiO_3$. A corresponding SAED pattern can be observed in Figure 2C, with the diffraction rings attributable to $SrTiO_3$.

The 40 nm $SrRuO_3$ sample is shown in Figure 2D-F. A SEM image can be seen in Figure 2D and is suggestive of the rather uniform nanoparticulate size distribution of 37.3 nm. The high resolution image (Figure 2E) corroborates the crystalline nature of the material, with a calculated *d*-spacing of 2.00 Å, corresponding to the (220) plane of $SrRuO_3$. A SAED pattern can be found in Figure 2F and is indicative of $SrRuO_3$.

Figure 2G-I can be ascribed to the larger $SrTiO_3$ sample. In particular, Figure 2G shows a mean particle size of 113 ± 40 nm. The HRTEM image in Figure 2H reinforces a *d*-spacing value

of 2.74 Å, which is associated with the (110) plane of $SrTiO_3$. Additionally, the SAED pattern in 2I further supports the claim that $SrTiO_3$ was synthesized.

Figure 2J-L refers to the larger $SrRuO_3$ sample, with a corresponding SEM image given in Figure 2J. The average particle size of our as-synthesized NPs is 146 ± 49 nm. Analysis of the HRTEM image in Figure 2K is consistent with a *d*-spacing of 1.98 Å, which can be ascribed to the (220) plane of $SrRuO_3$. The SAED pattern in Figure 2L is also indexed and maintains diffraction rings that can be linked with $SrRuO_3$.

Material	Size (nm)	BET Surface Area (m^2/g)	Synthesis Method	Ref
TiO_2	12 ± 3	130	Hydrothermal, 170°C	28
RuO_2	12 ± 3	42 ± 2	Polymerization, 400°C	29
RuO_2	N/A	36	Commercial (Alfa Aesar)	30
$SrTiO_3$	20-50	27.96	Hydrothermal, 200°C	31
$SrTiO_3$	55	26.4	Polyacrylamide gel , 550°C	32
$SrTiO_3$	24-40	30 to 50	Commercial	N/A
$SrTiO_3$	60-200	5 to 10	Commercial	N/A
$SrRuO_3$	126 ± 45	11.427	Molten Salt, 700°C	16
$SrRuO_3$	N/A	9	Solution Combustion	14
$SrRuO_3$	N/A	6 to 17	Annealing, 300-1000°C	14

Table S1. Table of metal oxide/perovskite materials synthesized from the prior literature with their corresponding sizes, BET surface areas, and synthesis methods.

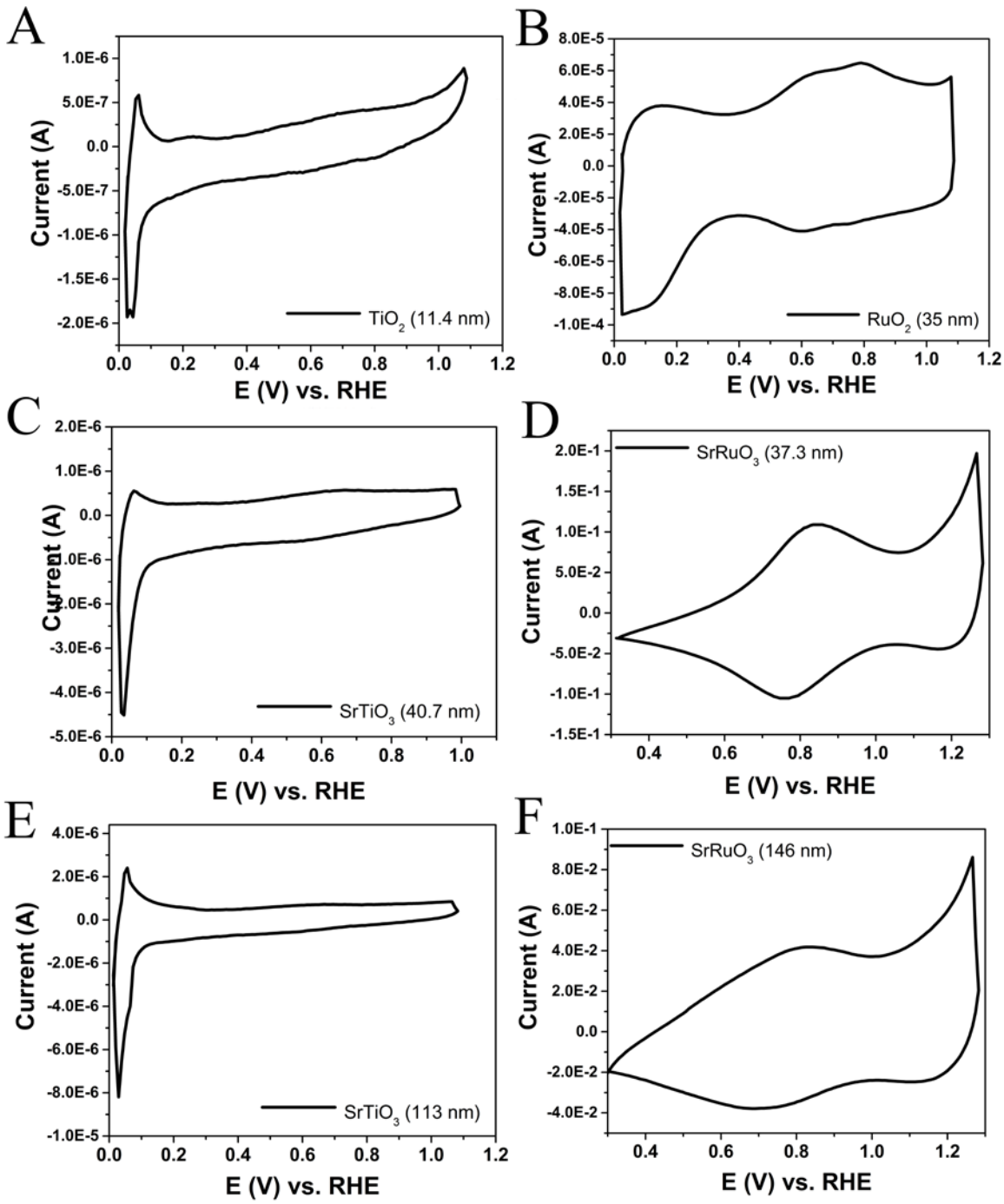

Figure S2. Cyclic voltammograms in an argon-saturated 0.1 M H_2SO_4 solution, obtained at a scan rate of 20 mV/s for (A) TiO_2 NPs (11.4 nm), (B) RuO_2 NPs (35 nm), (C) $SrTiO_3$ NPs (40.7 nm), (D) $SrRuO_3$ NPs (37.3 nm), (E) $SrTiO_3$ NPs (113 nm), and (F) $SrRuO_3$ NPs (146 nm), respectively.

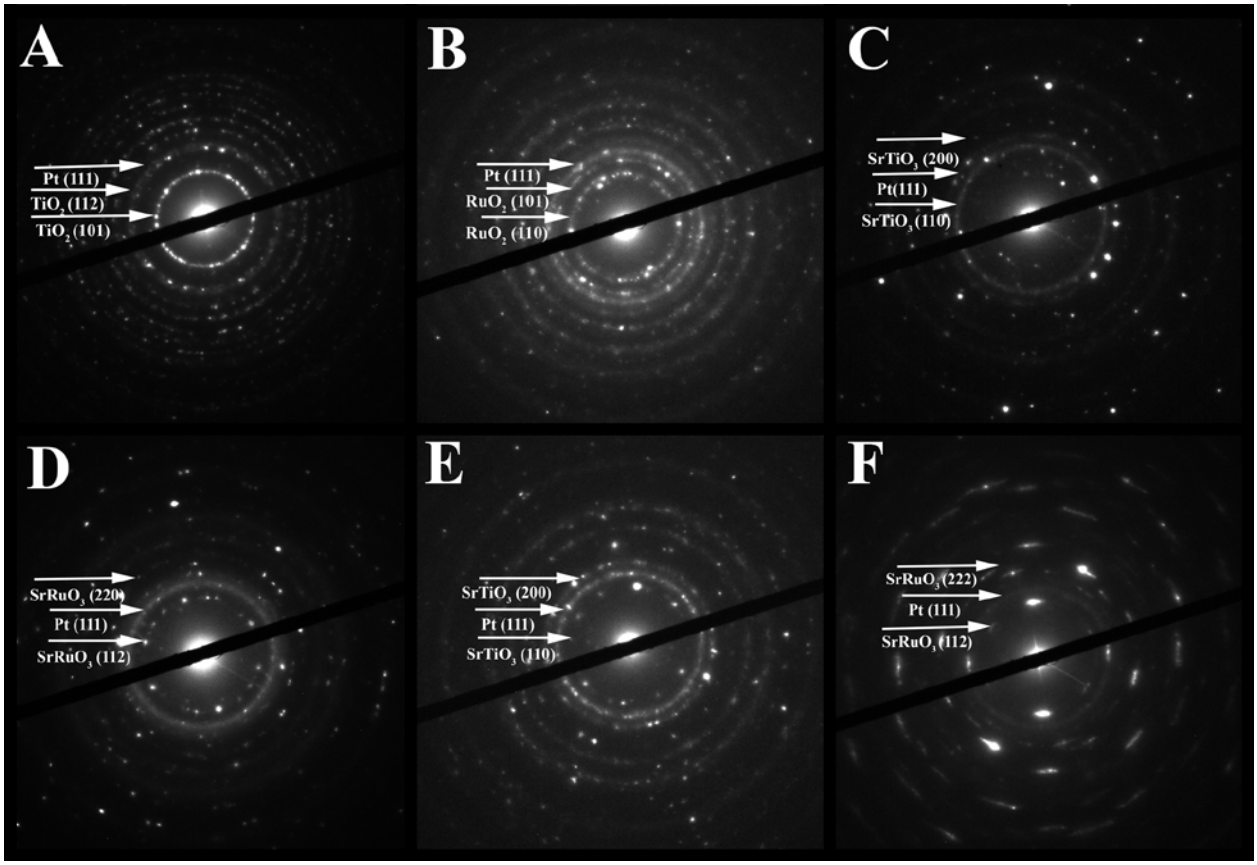

Figure S3. Single area electron diffraction patterns of (A) Pt/TiO_2 NPs (11.4 nm), (B) Pt/RuO_2 NPs (35 nm), (C) Pt/$SrTiO_3$ NPs (40.7 nm), (D) Pt/$SrRuO_3$ NPs (37.3 nm), (E) Pt/$SrTiO_3$ NPs (113 nm), and (F) Pt/$SrRuO_3$ NPs (146 nm), respectively.

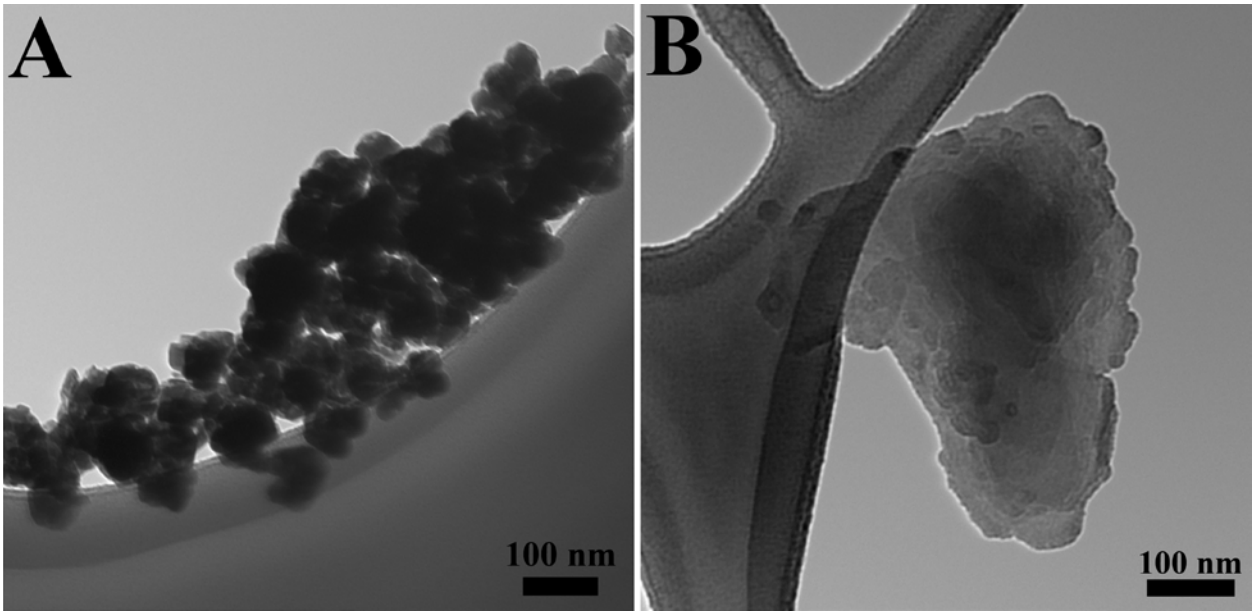

Figure S4. TEM images of (A) $SrRuO_3$ NPs (37.3 nm), and of (B) $SrRuO_3$ NPs (146 nm), post stability testing, respectively.

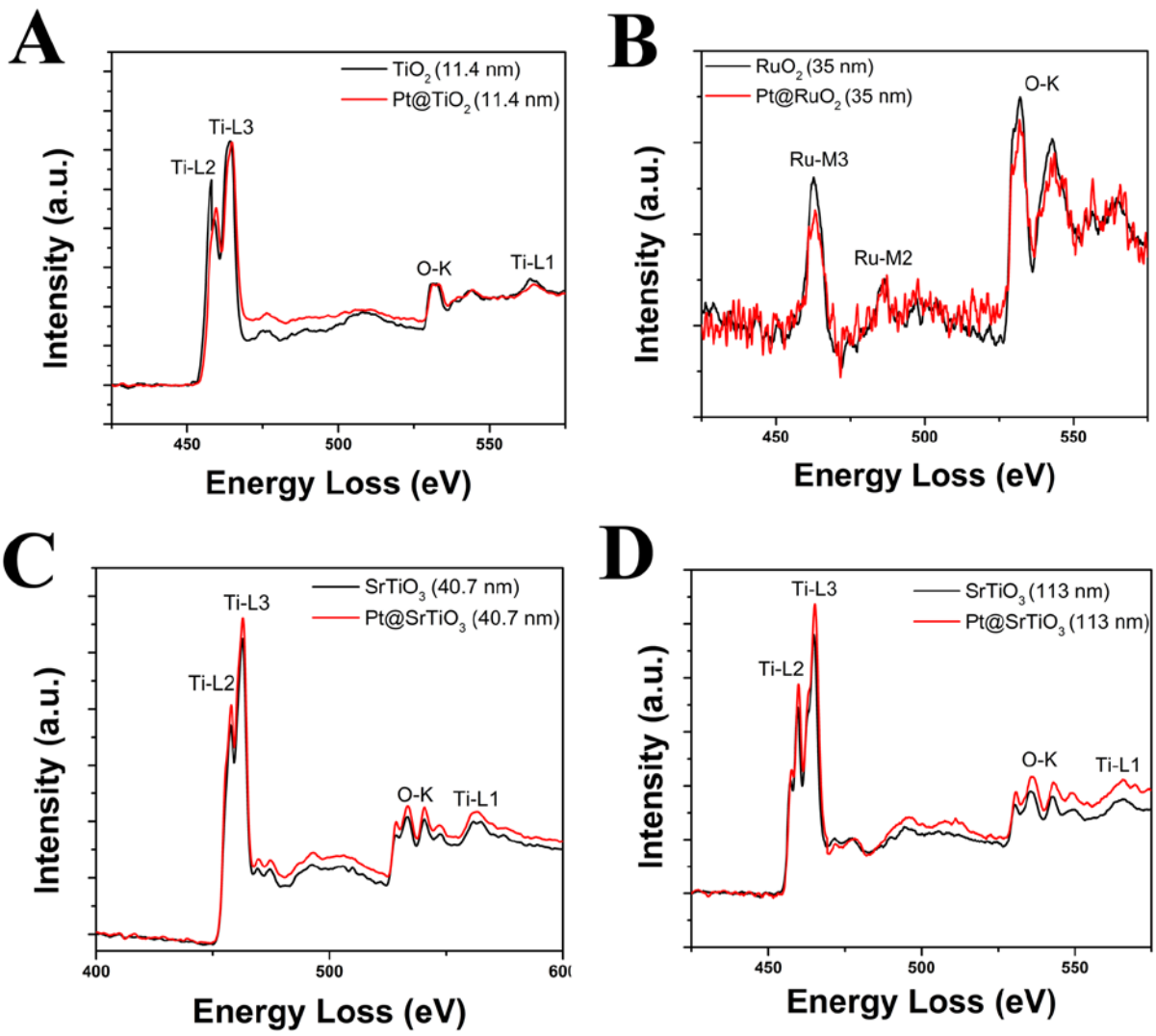

Figure S5. Electron energy loss spectra of (A) TiO_2 (red) and Pt/TiO_2 (black) (11.4 nm), (B) RuO_2 (red) and Pt/RuO_2 (black) (35 nm), (C) $SrTiO_3$ (black) and Pt/$SrTiO_3$ (40.7 nm) (red), and (D) $SrTiO_3$ (black) and Pt/$SrTiO_3$ (red) (113 nm), respectively.

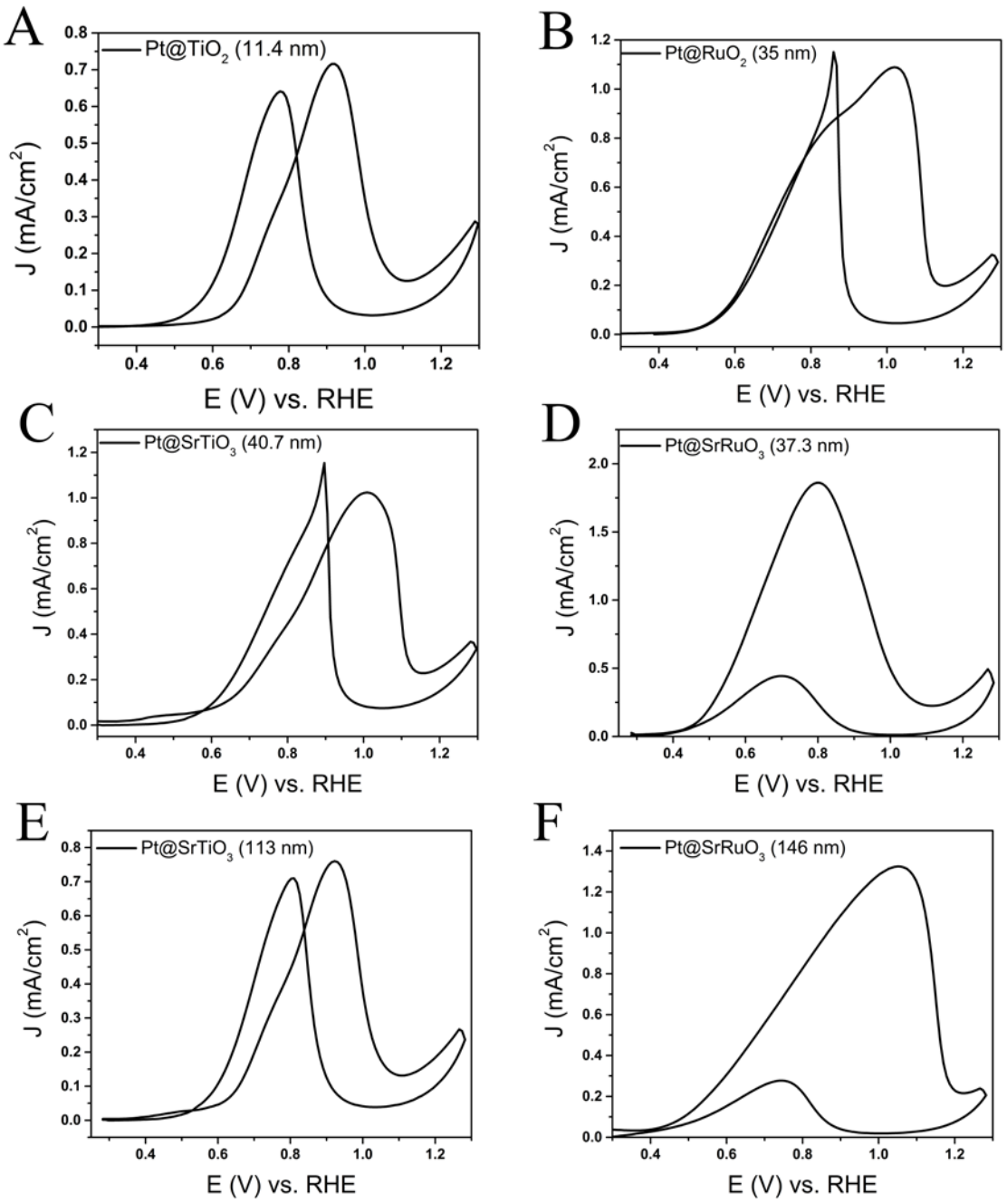

Figure S6. Full cyclic voltammograms for the methanol oxidation reaction acquired in an argon-saturated 0.1 M H_2SO_4 + 0.5 M MeOH solution for (A) Pt/TiO_2 NPs (11.4 nm), (B) Pt/RuO_2 NPs (35 nm), (C) Pt/$SrTiO_3$ NPs (40.7 nm), (D) Pt/$SrRuO_3$ NPs (37.3 nm), (E) Pt/$SrTiO_3$ NPs (113 nm), and (F) Pt/$SrRuO_3$ NPs (146 nm), respectively, obtained at a scan rate of 20 mV/s with the current normalized to the Pt ECSA.

Materials	Onset Potential (E (V) vs. RHE)	Activity vs. RHE (mA/cm^2)	Parameters	Reference
Pt/TiO_2 Nanotubes	0.67	0.2 @ 0.7 V	0.5 M H_2SO_4 + 1 M CH_3OH	*Applied Catalysis B: Environmental* **106** (2011) 609–615
Pt/TiO_2 substrate	0.52	1.1 @ 0.88 V	0.5 M H_2SO_4 + 0.5 M CH_3OH	*Nano Letters* **13** (2013) 4469−4474
Pt/WO_3/CNT	0.547	4.82 @ 0.83 V	1 M CH_3OH + 1 M H_2SO_4	*Journal of Materials Chemistry* **22** (2012) 16514-16519
Pt/RuO_2 film	~0.6	~0.032 @ 0.7 V	0.5 M H_2SO_4 + 0.1 M CH_3OH	*International Journal of Hydrogen Energy* **34** (2009) 2747–2757
Pt/RuO_2/Ti substrate	~0.5	~0.53 @ 0.7 V	0.1 M $HClO_4$ + 0.5 CH_3OH	*Chemistry Materials* **18** (2006) 5563-5570
$Pt/LaNiO_3$ Nanocubes	0.367	0.109 @ 0.81 V	0.1 M H_2SO_4 + 1 M CH_3OH	*Nanoscale* **4** (2012) 5386–5393
$Pt/LaNiO_3$ Powder	0.625	0.427 mA @ 0.865 V	0.5 M H_2SO_4 + 1 M CH_3OH	*Journal of Power Sources* **185** (2008) 670–675
$Pt/p\text{-}H_xMoO_3$	~0.37	0.55 @ 0.96 V	0.5 M H_2SO_4 + 1 M CH_3OH	*Journal of Power Sources* **259** (2014) 255-261
Pt/TiN Nanotubes	0.537	0.87 @ 0.797 V	1 M CH_3OH + 0.5 M H_2SO_4	*Electrochimica Acta* **141** (2014) 279–285
$Pt/C\text{-}Sm_2O_3$	~0.6	0.145 @ 0.9 V	2.0 M CH_3OH + 1.0 M H_2SO_4	*Electrochimica Acta* **54** (2009) 3103–3108

Table S2. Table describing relevant metal oxide support systems tested as well as their corresponding methanol oxidation onset potentials and specific activities.

Material	Size (nm)	Pt ECSA (cm^2)
TiO_2	11.4	9.29
RuO_2	35	1.79
$SrTiO_3$	40.7	4.81
$SrRuO_3$	37.3	7.45
$SrTiO_3$	113	4.31
$SrRuO_3$	146	3.35

Table S3. Calculated Pt electrochemically active surface area on each substrate tested, normalized for the same amount of Pt used for each sample.